

**Table VI.** Differences between the C-D and C-H Bond Moments (D) from Isotopically Substituted Species of Cyclohexane

isotopomer	dipole component	bond moment
CH- $d_2$	$\mu_c$	0.0081
CH- $d_1$ -eq	$\mu_c$	0.0069
CH- $d_6$	$\mu_b$	0.0115
	$\mu_c$	0.0079

than 0.005 Å except for the C-H bond lengths determined by electron diffraction which are substantially longer. The angles are consistent within 2°. Much better agreement is observed between the angles of the substitution structure and those from the ab initio calculation with the 4-31G basis set.<sup>9</sup> From our results, we found that the axial C-H bonds are not exactly parallel to the molecular symmetry axis but are tilted away from it by an angle of 1.5°.

The axial and equatorial C-H bond lengths and CCH angles of the substitution structure are different in the same sense as predicted from the ab initio calculation. However, the difference of the  $r_e$  bond lengths of 0.008 Å is much larger than the expected  $r_e$  difference of 0.002 Å. An independent estimate of this difference was obtained from the correlation between C-H stretching frequencies and corresponding bond lengths given by McKean.<sup>36</sup> Caillod et al.<sup>37</sup> determined the stretching frequencies of cyclo-

hexane  $\nu(\text{C-H}_{\text{eq}})$  to be larger than  $\nu(\text{C-H}_{\text{ax}})$  by 31  $\text{cm}^{-1}$ . This leads to a difference in the bond lengths of 0.003 Å, which is closer to the values from the ab initio calculations. A similar exaggeration of the difference between in-plane and out-of-plane C-H bond lengths in the methyl group of acetaldehyde was observed previously for the substitution structure.<sup>30</sup>

It will be assumed that the small vibrationally induced electric dipole moment of the isotopomers of cyclohexane studied here originates from equal contributions along each C-D bond. By using the substitution structure, the measured  $\mu_b$  and  $\mu_c$  dipole components are converted to an effective difference between the C-H and C-D bond moment. The results listed in Table VI show a considerable scatter with a mean value of 0.0086 D. Fliege and Dreizler<sup>16</sup> collected a list of such differences which range from 0.0031 to 0.0141 D for eight molecules studied so far. Our mean value fits nicely in this range.

**Acknowledgment.** Financial support by the Schweizerischer Nationalfonds (Project No. 2.005-0.86 and 20-5482.88) is gratefully acknowledged. We thank Dr. B. Vogelsanger for his help with the measurements and Professor I. Ozier for critically reading and improving the manuscript.

**Registry No.** CH- $d_0$ , 110-82-7; CH- $d_1$ , 26168-37-6; CH- $d_2$ , 33744-45-5; CH- $^{13}\text{C}$ - $d_2$ , 124382-54-3; CH- $d_6$ , 2652-64-4.

**Supplementary Material Available:** Listings of measured rotational frequencies of CH- $d_2$ , CH- $^{13}\text{C}$ - $d_2$ , CH- $d_1$ -eq, CH- $d_1$ -ax, and CH- $d_6$  (Tables VII-XI) (6 pages). Ordering information is given on any current masthead page.

(36) McKean, D. C. *Chem. Soc. Rev.* **1978**, 7, 399-422.

(37) Caillod, J.; Saur, O.; Lavalley, J.-C. *Spectrochim. Acta A* **1980**, 36, 185-191.

## Electron Tunneling in a Cofacial Zinc Porphyrin-Quinone Cage Molecule: Novel Temperature and Solvent Dependence

John K. Delaney,<sup>†</sup> David C. Mauzerall,<sup>\*,†</sup> and Jonathan S. Lindsey<sup>‡</sup>

Contribution from The Rockefeller University, 1230 York Avenue, New York, New York 10021, and Department of Chemistry, Carnegie Mellon University, Pittsburgh, Pennsylvania 15213.

Received January 9, 1989

**Abstract:** The zinc porphyrin-quinone cage molecule ZnPQ(Ac)<sub>4</sub> exists as two slowly equilibrating conformers differing in the interplanar porphyrin-quinone distance and thus in the size of the cavity. The close conformer, PQ<sub>a</sub>, shows only a 4-fold change in rate of quenching of fluorescence in 21 solvents of widely varying properties. Rate constants have been measured in four solvents over wide ranges of temperature: 300-80 K. The activation energies in five solvents are small, varying between -1 and +2 kJ/mol. The quenching rates of the singlet state of the more distant conformer PQ<sub>b</sub> vary over a somewhat greater range (10-fold) in these solvents with activation energies of +4 kJ/mol. The activation energies of the forward and reverse electron transfer from the triplet state average +7 kJ/mol. The rates are little affected by viscosity including transition to the glassy state. The weak temperature and solvent dependence of electron transfer in ZnPQ(Ac)<sub>4</sub> can best be explained by nonadiabatic electron tunneling. The triplet reaction stores >90% of the energy of the excited state in the free energy of the products. The interesting observation was made that increasing the molar volume of the solvent decreased the conformer equilibrium constant.

The determination of the structure of the bacterial photosynthetic reaction centers by X-ray crystallography<sup>1,2</sup> has focused efforts to explain and duplicate their remarkable efficiency. A striking characteristic of the reaction center is the spacing of the molecules (except for the primary donor, a dimer of bacteriochlorophyll) at about 5 Å beyond the van der Waal's radii. This is close to the optimum distance predicted for electron tunneling reactions.<sup>3</sup> A characteristic of this transfer mechanism is its temperature independence.<sup>4,5</sup> Several porphyrin quinone mole-

cules with varying degrees of structural rigidity and porphyrin-quinone separation have been prepared and their photophysical properties determined.<sup>6</sup> However, little work has been done on

(1) Disenhofer, J.; Epp, O.; Miki, K.; Huber, R.; Michel, H. *Nature* **1985**, 318, 618-624.

(2) Allen, J. P.; Feher, G.; Yeats, T. O.; Komiya, H.; Rees, D. C. *Proc. Natl. Acad. Sci. U.S.A.* **1987**, 84, 5730-5734 and 6162, 6166.

(3) Mauzerall, D. *Brookhaven Symposia in Biology* **1976**, 28 64-73. Mauzerall, D. In *Photoinduced Electron Transfer*; Fox, M. A., Chanon, M., Eds.; Elsevier: Amsterdam, 1988; Part A, Chapter 1.6, pp 228-244.

(4) Devault, D.; Chance, B. *Biophys. J.* **1966**, 6, 825-847.

(5) McElroy, J. D.; Mauzerall, D.; Feher, G. *Biochim. Biophys. Acta* **1974**, 333, 261-277.

<sup>†</sup>The Rockefeller University.

<sup>‡</sup>Carnegie Mellon University.

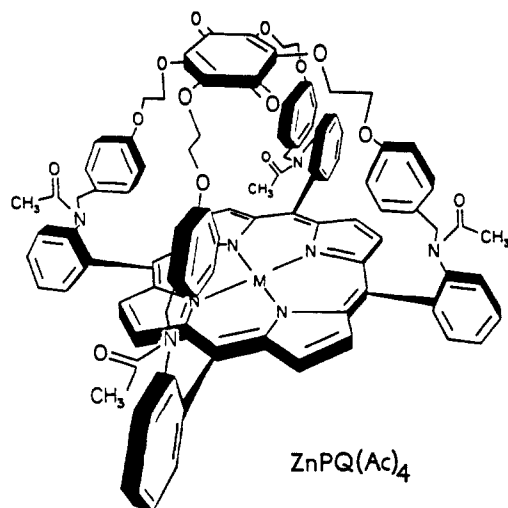


Figure 1. Structure of  $\text{ZnPQ}(\text{Ac})_4$ ,  $M = \text{Zn}$ .

solvent and particularly on temperature dependencies of the electron transfer.

The most comprehensive study of solvent effects was carried out on tetraphenylporphyrin–amide–quinone.<sup>7</sup> The electron-transfer rate, estimated from the fluorescence lifetime, ranged over 50-fold in 22 solvents. The rate constants were roughly correlated by the Onsager–Mataga–Ottolenghi equation implying an optical or Franck–Condon transition for the electron transfer. Interpretations of solvent effects on electron-transfer reactions have usually stressed energetics, the stabilization of the charged species in polar solvents<sup>8</sup> and, more recently, the influence of solvent dynamics on rapid reactions.<sup>9</sup> Our results, on an equally large selection of solvents, show such effects are small and overall are in better agreement with the results on the porphyrin–amide–quinone.

Unfortunately, far less work has been done on the temperature dependence of electron-transfer reactions. A recent review<sup>10</sup> shows poor correlation with Marcus theory, although most of the data covers a small temperature range (50 °C). The observed activation energies of the fluorescence quenching of aromatic molecules are often appreciable (15–30 kJ mol<sup>-1</sup>). Evidence for electron transfer in a zinc porphyrin–phenyl–bicyclooctane–quinone<sup>11</sup> at 77 K and in a zinc porphyrin–tryptycene–tetracyanonaphthoquinodimethane<sup>12</sup> at 10 K has been obtained. Our more extensive studies in several solvents and over a wide range of temperature (200 °C) show that the temperature effects can be very small indeed.

We have prepared a cofacial zinc porphyrin–quinone cage molecule,  $\text{ZnPQ}(\text{Ac})_4$  (Figure 1), which has the following photochemical features:<sup>13</sup> (1) The decreased fluorescence yield and shortened fluorescence lifetime of  $\text{ZnPQ}(\text{Ac})_4$ , relative to reference zinc porphyrins, results from electron-transfer interactions. The quantum yield of these electron-transfer interactions is 60% in polar solvents. (2) The biphasic fluorescence decay of  $\text{ZnPQ}(\text{Ac})_4$  is attributed to introverted  $\text{PQ}_a$  and extroverted  $\text{PQ}_b$  conformeric forms with porphyrin–quinone interplanar center-to-center dis-

Table I. Solvent Dependence of Singlet State Electron-Transfer Time Constants and Conformer Equilibrium<sup>a</sup>

solvent	$\epsilon$	$n^2$	$\tau_a$ , ns	$\tau_b$ , ns	$K$
benzene	2.27	2.24	1.8	>50	1.22
toluene	2.38	2.23	1.6	>50	1.40
hexafluorobenzene		1.90	0.9	>50	0.6
diethyl ether	4.33	1.82	1.72	30	1.38
ethyl acetate	6.02	1.88	1.96	10	1.00
tetrahydrofuran	7.58	1.97	1.40	8	1.50
carbon tetrachloride	2.24	2.12	0.52	6.8	0.35
pentachloroethane	3.73	2.26	0.96	6.4	0.37
1,1,2,2-tetrachloroethane	8.20	2.22	0.84	5.4	2.13
1,1,1-trichloroethane	7.25	2.06	0.66	6.7	0.2
1,1,2-trichloroethane	7.29	2.16	1.07	6.3	1.04
1,2-dichloroethane	10.36	2.08	0.81	7.4	1.86
methylene chloride	8.93	2.02	0.92	6.6	1.78
chloroform	4.80	2.08	0.79	6.3	2.03
sucrose octaacetate		2.15	1.29	>50	1.22
pyridine	12.9	2.27	0.63	13	4.0
ethanol	24.5	1.85	0.63	13	5.7
acetonitrile	35.9	1.80	0.63	3.0	1.5
dimethylacetamide	37.8	2.06	0.55	13	4.0
dimethyl sulfoxide	46.7	2.18	0.63	13	5.7
average spacer of PQ	22	2.39			

<sup>a</sup>Solvent constants were obtained from standard sources such as Riddick, Bunger, and Sakano<sup>33</sup> and Maryott and Smith.<sup>34</sup> The properties of the average spacer were calculated as equimolar mixtures of 4-methylanisole and *N*-methyl-*N*-phenylacetamide ( $n^2$ ) and of anisole and dimethylacetamide ( $\epsilon$ ).

tances of 6.5 and 8.5 Å, respectively.<sup>13,14</sup> The electron transfer or interaction time constants are 0.6 and 13 ns, respectively, in polar solvents. (3) The triplet states undergoes electron transfer with risetime of 150 ns and decay of the charge-separated state with lifetime of 1.4 μs in polar solvents. The quantum yield of triplet state formation is 30%, and the yield of triplet electron transfer is unity.

We now present our data on the effects of solvent and temperature on the electron-transfer reactions of this compound. We find that the effects of both solvent and temperature are small and are best explained by nonadiabatic electron tunneling. The  $\text{ZnPQ}(\text{Ac})_4$  cage molecule is sufficiently enclosed that the electron-transfer reaction is largely independent of its solvent environment.

## Experimental Section

Fluorescence lifetimes were measured with an error of  $\pm 0.04$  ns by using a 300 ps  $\text{N}_2$  laser pulse at 337 nm and a scan converter.<sup>13,15</sup> Occasionally a homemade dye laser was added to obtain excitation at 560 nm. Typically 64 pulses were averaged at 2 pps. The data were fit by least-squares iterative convolution.<sup>15,16</sup> Low-temperature fluorescence measurements were performed by using a long-necked 1-cm<sup>2</sup> fused quartz fluorescence cuvette with rounded edges (Precision Cells), a liquid  $\text{N}_2$  cooled cryostat (Oxford Systems Inc.), and a homemade regulating circuit. The cryostat and regulating circuit have a temperature drift of less than 1 K over a 15–20 min span. The sample was allowed to equilibrate at each temperature for 10 min. No hysteresis was detected. All solvents were of spectroscopic or HPLC quality. The sucrose octaacetate was recrystallized from ethanol to remove yellow and fluorescent impurities. Samples ( $2 \times 10^{-6}$  M) were flushed with  $\text{N}_2$  for 10 min prior to experimentation. No deterioration in the  $\text{ZnPQ}(\text{Ac})_4$  sample following fluorescence determinations was detected by absorption spectroscopy and by HPLC.

A diode-array pulsed spectrometer (DAPS) was used for flash photolysis with a time resolution of 20 ns and a spectral resolution of 2.5 nm over a range of 200 nm.<sup>17</sup> Excitation was performed with a 15 ns pulse at 561 nm (1 mJ) from a XeCl excimer pumped dye laser (Lamda Physik

(14) A high-field NMR study shows that a helical twisting of the bridging chains occurs. The configuration of the oxyethyleneoxy moieties is consistent with that of the two conformers. Lisicki, M. A.; Mishra, P. K.; Bothner-By, A. A.; Lindsey, J. S. *J. Phys. Chem.* **1988**, *92*, 3400–3403.

(15) Mauzerall, D. C. *Biochim. Biophys. Acta* **1985**, *809*, 11–16.

(16) Demas, J. N. *Excited State Lifetime Measurements*; Academic Press: New York, 1983.

(17) Sedlmair, J.; Ballard, S. G.; Mauzerall, D. *Rev. Sci. Instrum.* **1986**, *57*, 2995–3003.

(6) Connolly, J. S.; Bolton, J. R. In *Photoinduced Electron Transfer*; Fox, M. A., Chanon, M., Eds.; Elsevier: Amsterdam, 1988; Part D, Chapter 6.2, pp 303–393.

(7) Schmidt, J. A.; Siemiarczuk, A.; Weedon, A. C.; Bolton, J. R. *J. Am. Chem. Soc.* **1985**, *107*, 6112–6114.

(8) Santamaria, J. In *Photoinduced Electron Transfer*; Fox, M. A., Chanon, M., Eds.; Elsevier: Amsterdam, 1988; Part B, pp 483–540.

(9) Calef, D. F. In *Photoinduced Electron Transfer*; Fox, M. A., Channon, M., Eds.; Elsevier: Amsterdam, 1988; Part A, pp 362–390.

(10) Baggott, J. E. In *Photoinduced Electron Transfer*; Fox, M. A., Chanon, M., Eds.; Elsevier: Amsterdam, 1988; Part B, pp 385–419.

(11) Leland, B. A.; Joran, A. D.; Felker, P. M.; Hopfield, J. J.; Zewail, A. H.; Dervan, P. B. *J. Phys. Chem.* **1985**, *89*, 5571–5573.

(12) Wasielewski, M. R.; Johnson, D. G.; Svec, W. A.; Kersey, K. M.; Minsek, D. W. *J. Am. Chem. Soc.* **1988**, *110*, 7219–7221.

(13) Lindsey, J. S.; Delaney, J. K.; Mauzerall, D.; Linschitz, H. *J. Am. Chem. Soc.* **1988**, *110*, 3610–3621.

Table II. Temperature Dependence of Excited State Reactions: Electron-Transfer Activation Energies and Conformer Equilibrium Enthalpies

solvent	temp range, K	$\Delta H^\circ$ , kJ/mol K	$E_a$ , kJ/mol			
			singlet		triplet	
			$k_a$	$k_b$	$k_T^a$	$k_{P^+}^b$
ethanol-methanol (4:1)	300-190	+9.7 $\pm$ 1.2	-0.9 $\pm$ 0.2	+0.2 $\pm$ 0.3	+5.5 $\pm$ 0.2 <sup>a</sup>	+10 $\pm$ 1 <sup>a</sup>
	190-80	freeze out		+4.2 $\pm$ 0.2		
dimethylacetamide-ethanol (1:1)	290-125	+3.8 $\pm$ 0.8	0 $\pm$ 1	+4 $\pm$ 2		
dichloromethane	300-190	-3.4 $\pm$ 0.8	+1.7 $\pm$ 0.8	+2.7 $\pm$ 0.4	+6.7 $\pm$ 0.8	+6.7 $\pm$ 1
toluene	300-225	+6.7 $\pm$ 5.0	-1 $\pm$ 1		+6.3 $\pm$ 1	
	225-180	freeze out				
sucrose-octaacetate	300-190	+3.8 $\pm$ 0.4	-0.4 $\pm$ 0.2			
	190-80	freeze out				

<sup>a</sup> The activation energy for  $k_T^a$  is 3.5  $\pm$  1 kJ/mol and for  $k_{P^+}^b$  is 5.5  $\pm$  1 kJ/mol.

50E, F1-2000). A pulsed N<sub>2</sub> laser (Moletron UV1000) was used to excite a mixture of Coumarin 440, PPO, and Rhodamine 590 in methanol, and the resulting broad band fluorescence was used as the measuring pulse. Data acquisition and analysis were done with a DATA 6000 digitizer (Analogic) and a HP86B computer (Hewlett Packard). Samples were purged for 30 minutes with N<sub>2</sub> via a metal and glass coaxial system.<sup>18</sup> Typically 64-128 data sets were collected for each difference spectrum. No sample deterioration was detected by absorption spectroscopy and HPLC at the end of an experiment.

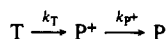
**Data Analysis. Singlet State.** The fluorescence lifetime data were analyzed as originating from two nonequilibrating conformers of ZnP\*Q(Ac)<sub>4</sub>. Evidence for this assumption was presented previously.<sup>13</sup> The lifetimes of the two conformers are obtained from the biexponential decays, and the ratio of their amplitudes is the ratio of the two conformers, i.e., the equilibrium constant,  $K = PQ_a/PQ_b$ . The observed rate constants ( $1/\tau_1$ ,  $1/\tau_2$ ) are the sum of electron-transfer constant ( $1/\tau_a$ ,  $1/\tau_b$ ) plus the usual decay channels of the singlet state of the porphyrin without a quinone ( $1/\tau_0$ ):

$$k_a = 1/\tau_a = 1/\tau_1 - 1/\tau_0 \quad (1)$$

$$k_b = 1/\tau_b = 1/\tau_2 - 1/\tau_0 \quad (2)$$

It is worth noting the alternative explanation where PQ<sub>b</sub> converts to PQ<sub>a</sub> which then rapidly undergoes electron transfer. In this case  $k_b$  approaches zero, and  $k_a$  is greater than the conformer interconversion rate constant,  $k_i$ . The amplitudes of the fluorescence decay retain their previous interpretations, but now  $k_b$  becomes the interconversion rate constant,  $k_i$ . The fact that the observed  $k_{b,i}$  is slower in nonpolar solvents and in general tracks  $k_a$  (Table I) indicates that the measured  $k_{b,i}$  is the actual electron-transfer rate constant and not the interconversion rate. Furthermore, the observation of a second, slower component in triplet state reaction (see below) effectively rules out this possibility. The interconversion rate is slow on the time scales of interest,  $<10^{-4}$  s.

**Triplet State.** For the simple kinetic scheme



the observed absorbance change at a given wavelength following  $\delta$  function excitation of P to T, will be

$$\Delta A/T_0 = [\Delta\epsilon_T - \Delta\epsilon_{P^+}k_T/(k_T - k_{P^+})]e^{-k_T t} + [\Delta\epsilon_{P^+}k_T/(k_T - k_{P^+})]e^{-k_{P^+} t} \quad (3)$$

where  $\Delta A/T_0$  is the normalized change in absorbance,  $\Delta\epsilon_T = \epsilon_T - \epsilon_P$  and  $\Delta\epsilon_{P^+} = \epsilon_{P^+} - \epsilon_P$ . At a zero crossing of the triplet and ground-state spectra ( $\Delta\epsilon_T = 0$ ), there will be a single exponential rise with constant  $k_T$  and a single exponential fall with constant  $k_{P^+}$ . This is observed near 415 nm in polar solvents (Figure 4A). At most other wavelengths,  $\Delta\epsilon_T$  is somewhat greater than  $\Delta\epsilon_{P^+}$ . Since  $k_T$  is about  $10k_{P^+}$ , the observed result will be a monotonic decay of the absorption change with a small amplitude component of rate constant  $k_T$  and a major component of rate constant  $k_{P^+}$ . This is observed in the 470-nm region in all solvents (Figure 4A). At room temperature in ethanol-methanol, a third slower decay is seen and is assigned to the second conformer, PQ<sub>b</sub>. Since these components differ in time by orders of magnitude (Table III), they are readily separated.

A sensitive method of analyzing flash photolysis data is to plot ratios of absorbance changes at differing wavelengths<sup>19</sup> as a function of time. The number of components in a system can be determined by the number

of differing wavelength ratios required for constancy. For the three-component system of eq 3, a plot of ratio of absorbancies at two wavelengths versus time will only be constant when  $k_T = k_{P^+}$  or when  $\Delta\epsilon_T^{\lambda_1} \times \Delta\epsilon_{P^+}^{\lambda_2} = \Delta\epsilon_{P^+}^{\lambda_1} \times \Delta\epsilon_T^{\lambda_2}$ . The former case is ruled out by single wavelength plots, but the second case fits the data at some wavelengths. In general, a monotonic increase or decrease of the ratio to a constant level (only P<sup>+</sup> and P present) is predicted. Thus the observation of a second change in the ratio plot versus time following its rise to a plateau (Figure 4B) clearly implicates more than three components. This was generally seen when  $\Delta\epsilon_{P^+} \gg \Delta\epsilon_T$ , i.e., when the ratio of wavelengths included 415 nm. We assign this fourth component to the triplet of PQ<sub>b</sub> by the following argument. In principle, four rate constants are observable if the interconversion rate is slow: that of formation and decay of P<sup>+</sup>Q<sup>-</sup> for each of the two conformers. Both the forward rate constant ( $k_T^a$ , the formation of P<sup>+</sup>Q<sub>a</sub><sup>-</sup> from the triplet PQ<sub>a</sub>) and the reverse constant ( $k_{P^+}^b$ , the decay of P<sup>+</sup>Q<sub>a</sub><sup>-</sup> to the ground state, PQ<sub>a</sub>) are unambiguously resolved by the rise and fall of the 415-nm band at higher temperatures (Figure 4A). The decay at 470 nm can be resolved into at least three and possibly four components. The fastest decay component at 470 nm with time constant equal to the rise at 415 nm is  $k_T^a$ . The next component has time constant equal to the fall of the 415-nm band and is assigned to  $k_{P^+}^b$ . The third component is assigned to  $k_T^b$  since it is some 20-fold slower than  $k_T^a$ , which is the same ratio of rates as seen in the singlet state (Table I). The fourth component is assigned to  $k_{P^+}^c$ , the decay of P<sup>+</sup>Q<sub>b</sub><sup>-</sup>. The limited S/N and extent of the data do not allow all four time constants to be resolved at all temperatures. However, at least two components are seen at all temperatures. The present analysis is consistent with all of our data, but, as with interpretations of kinetic data, it may not be unique.

## Results

**1. Singlet State. (a) Solvents.** The fluorescence lifetime of the reference porphyrin, ZnPA<sub>4</sub>(Ac)<sub>4</sub>, was invariant with solvent, indicating the intersystem crossing rate, internal conversion rate, and radiation rate constants do not change with solvent.<sup>13</sup> The electron-transfer time constants ( $\tau_a$ ,  $\tau_b$ ) and equilibrium constants ( $K$ ) of the two conformers of ZnPQ(Ac)<sub>4</sub> (Table I) in 21 solvents at room temperature were determined from the fluorescence lifetimes and amplitudes.

**(b) Temperature.** The fluorescence lifetimes of the two reference porphyrins, ZnPA<sub>4</sub>(Ac)<sub>4</sub> (2.43 ns) and ZnPQH<sub>2</sub>(Ac)<sub>4</sub> (2.50 ns), were >95% monoexponential and were independent of temperature (298-83 K) in ethanol/methanol (4:1). Thus all the changes in lifetimes observed in ZnPQ(Ac)<sub>4</sub> can be ascribed to the electron-transfer reactions and to the conformer equilibria.

The electron-transfer rate constants and the equilibrium constants for the two conformers of ZnPQ(Ac)<sub>4</sub> are presented graphically for four solvents, ethanol/methanol (300-83 K, Figure 2), methylene chloride (298-188 K, Figure 3), toluene (298-183 K, Figure 3), and sucrose octaacetate (303-83 K, Figure 3). The same parameters were obtained on analysis of data obtained at the two emission bands showing the compounds to be homogeneous. The activation energies for electron transfer and the enthalpies for conformer interconversion are shown in Table II.

**Ethanol/Methanol (4:1).** The electron-transfer rate constant for PQ<sub>a</sub>,  $k_a$  increases by a factor of two between room temperature and that of liquid nitrogen (Figure 2). The rate constant for PQ<sub>b</sub>,  $k_b$ , is temperature independent from 300 to 200 K and then decreases to a value close to  $1/\tau_0$ , the observed fluorescence decay of reference porphyrins at 83 K. The activation energy is 4.2  $\pm$  0.2 kJ/mol. The equilibrium constant between the two conformers,

(18) Ballard, S. G.; Mauzerall, D. J. *Chem. Phys.* **1980**, *72*, 933-947.

(19) Mauzerall, D. J. *Am. Chem. Soc.* **1962**, *84*, 2437-2445.

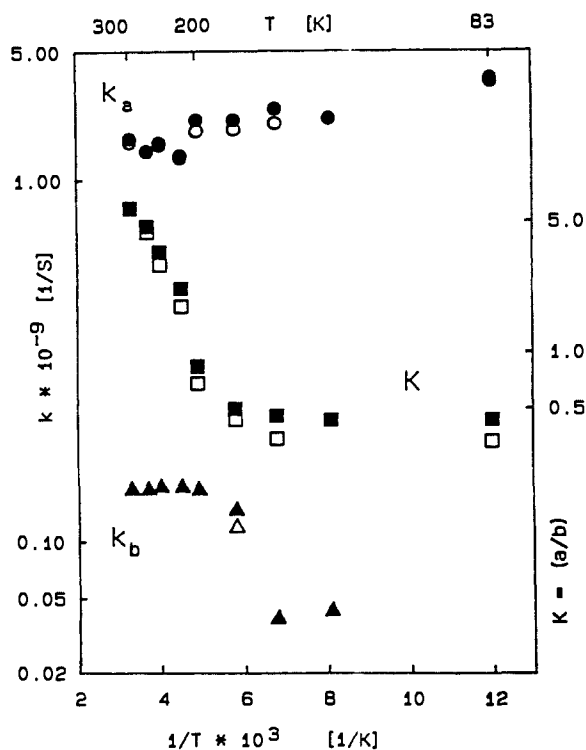


**Figure 2.** Temperature dependence of singlet state electron-transfer rate constants ( $\circ$ ,  $\bullet$   $k_a$ ;  $\Delta$ ,  $\blacktriangle$   $k_b$ ) and conformer equilibrium constant ( $\square$ ,  $\blacksquare$   $K$ ) in ethanol-methanol, 4:1 obtained from fluorescence lifetime measurements. The opened and closed symbols are data collected at 610 and 660 nm. Single symbols indicate identical values. Excitation wavelength was 337 nm.

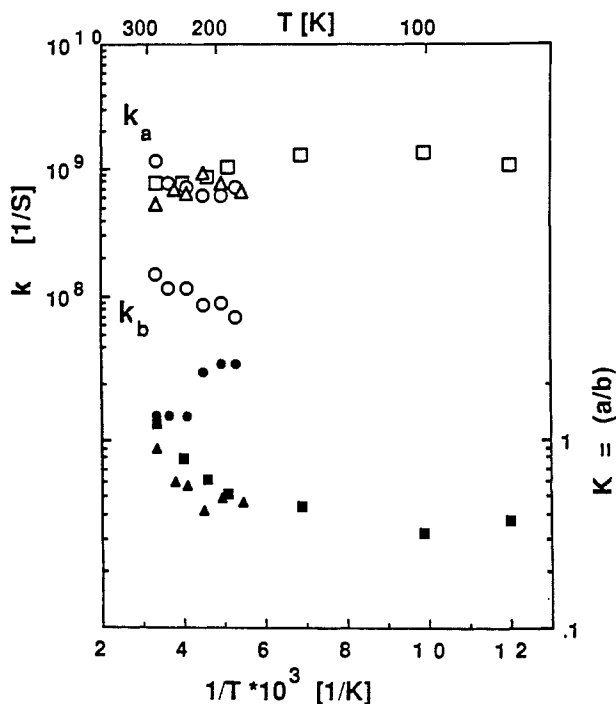


**Figure 3.** Temperature dependence of singlet state electron-transfer rate constants (open symbols,  $k_a$ ,  $k_b$ ) and the conformer equilibrium constant (closed symbols,  $K$ ) in methylene chloride ( $\circ$ ,  $\bullet$ ), toluene ( $\Delta$ ,  $\blacktriangle$ ), and sucrose octaacetate ( $\square$ ,  $\blacksquare$ ), obtained from fluorescence lifetime measurements. The excitation wavelength was 337 nm except sucrose octaacetate, 560 nm. The emission wavelength was 660 nm.

$K$ , exhibits a complementary behavior to  $k_b$ . Between 300 and 190 K the equilibrium shifts to favor  $PQ_b$  with an enthalpy of  $9.7 \pm 1.2$  kJ/mol. However, below 190 K the ratio remains constant indicating a freezing out of the equilibrium. The sharpness of the transition at 200 K suggests that the interconversion may be

**Table III.** Temperature Dependence of Triplet State Reaction<sup>a</sup>

temp, K	$T_{T_1}^a, \mu s$	$T_{P^+}^a, \mu s$	$T_{T_2}^b, ms$	$T_{P^+}^b, ms$	${}^3PQ_a/{}^3PQ_b$	triplet yield	
						measured	calcd
300	0.4	0.9	0.006	0.04	1.7	0.31	0.36
278	0.5	2.2			1.4	0.44	0.41
223	1.0	7.5			0.7	0.53	0.51
173	2.2	(30)	(0.03)	0.25	0.1	0.64	0.76
123			0.07	0.9	0.07	1.0	0.87
83			4	13	0.04	1	1

<sup>a</sup>Triplet yield and electron-transfer time constants in ethanol-methanol (4:1). The time constants and initially formed triplet yields were measured on the diode array pulse spectrometer as described in the Experimental Section. The time constants are assigned as described in the text. The data in parentheses are ambiguous since the Arrhenius plots cross at these temperatures. The triplet yields were calculated from the fluorescence data (Table II) as  $X_1\tau_1 + (1 - X_1)\tau_2$  and normalized to the value at 83 K. The yield of triplet at 83 K is 62% if the intersystem crossing time is 3 ns.

a cooperative process involving the four linkage groups.

**Methylene Chloride.** The rate constant  $k_a$  is essentially temperature independent (300–190 K), and  $k_b$  decreases 2-fold over this range (Figure 3). The equilibrium constant increases (i.e., increasingly favors  $PQ_a$ ) 2-fold over this range. The latter two dependencies are the opposite of those in the alcoholic solvent but are again complementary.

**Toluene.** In this nonpolar solvent  $k_a$  increases by only 40% over a similar range, 300–180 K. The equilibrium constant decreases 50% over the first half of the range and then remains constant (Figure 3). In this solvent  $\tau_2$  is close to that of the reference porphyrins and provides only a lower limit for  $\tau_b$  of 50 ns.

**Sucrose Octaacetate.** A distinction between temperature and viscosity effects can be drawn by using the near room temperature glass solvent, sucrose octaacetate. The rate constant  $k_a$  increases slightly with temperature over the range 300–80 K (Figure 3). The equilibrium constant decreases between 300 and 190 K and then is constant. The freezing out of the equilibrium occurs at about the same temperature (180 K) as in the alcoholic solvent. Thus the electron-transfer rate and the conformer equilibrium are independent of viscosity. As with toluene one can only quote a lower limit for  $\tau_b$  of 50 ns.

**2. Triplet State.** The similarity of the broadened spectra of the triplet state and cation makes their separation difficult by usual flash photolysis measurements.<sup>13</sup> The pulsed diode array spectrometer<sup>17</sup> allowed data acquisition of sufficient wavelength resolution to distinguish these species. The yield of triplet state at 300 K is about 25%, in agreement with the previous measurement.<sup>13</sup> The lifetime of triplet  $ZnPQH_2(Ac)_4$  in ethanol-methanol at 96 K is 14 ms. The lifetime of triplet  $ZnPA_4(Ac)_4$  is 14 ms at 173 K.

**Solvent and Temperature Effects. Ethanol/Methanol (4:1).** If all the observed rate constants are plotted versus reciprocal temperature, they cluster into four straight lines. This and the evidence given in the Experimental Section are the basis for the assignments shown in Table III. The activation energies are given in Table II. The ratio of the initially formed triplet states ( $PQ_a:PQ_b$ ) calculated from fluorescence lifetime data decreases from 1.7 at 300 K to 0.04 at 83 K and are in agreement ( $\pm 10\%$ ) with observation (Table III). This proves that electron transfer on charge recombination in the singlet state leads to the ground state not to the triplet.

The observed slow reaction of the triplet at low temperatures is not caused by the lack of reactivity of  $PQ_a$ , since its extrapolated time constant of  $80 \pm 20$  us at 80 K would be easily observable. It is rather the shift of the equilibrium to the  $PQ_b$  conformer and the inherently slower reactivity of the singlet  $PQ_b$  conformer together with its decreasing reactivity with decreasing temperature that limits the observation of electron transfer at low temperature. The ratio of  ${}^3PQ_a$  to  ${}^3PQ_b$  decreases drastically with temperature if the conformer equilibration is slower than the reaction time scale. Since the equilibration time is long ( $> 10^3$  s) at 120 K, this assumption is reasonable.

**Methylene Chloride.** At room temperature the 415-nm band cannot be detected following excitation. The decay of the 470-nm

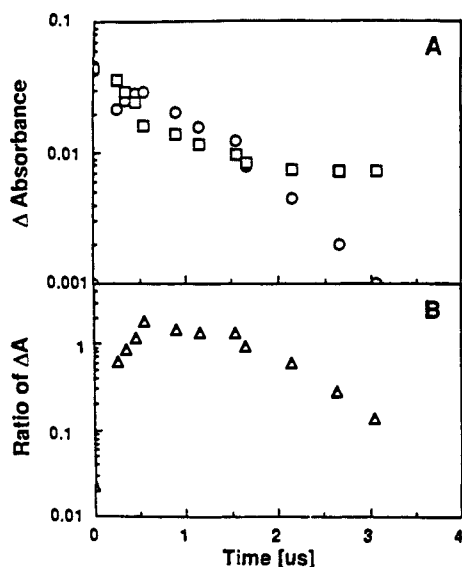


**Figure 4.** (A) Optical absorbance transients following flash photolysis of  $\text{ZnPQ}(\text{Ac})_4$  in ethanol-methanol 4:1 at 300 K: ( $\square$ ) 465 nm and ( $\circ$ ) 415 nm. (B) Ratio of absorbance change at 415 nm to that at 465 nm versus time following flash photolysis. Excitation pulse 15 ns at 560 nm,  $\sim 1 \text{ mJ cm}^{-2}$ .

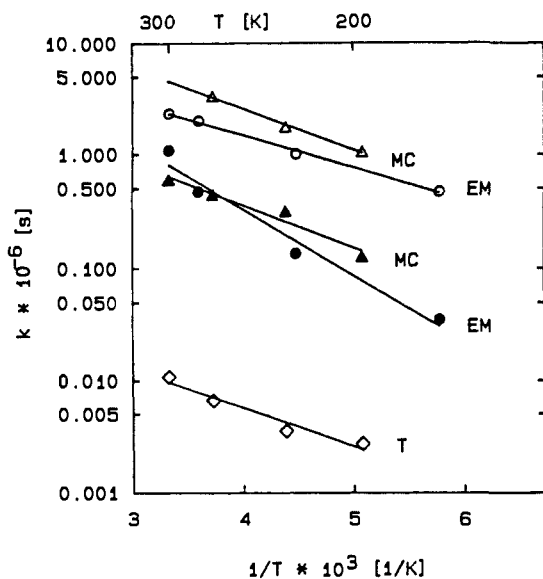


**Figure 5.** Temperature dependence of rate constants of electron transfer from the triplet state of  $\text{ZnPQ}(\text{Ac})_4$  (open symbols) and decay of  $\text{ZnP}^+\text{Q}^-(\text{Ac})_4$  (solid symbols) in various solvents: ( $\circ$ )  $k_T$  and ( $\bullet$ )  $k_{PT}$  in ethanol-methanol, 4:1 (EM); ( $\Delta$ )  $k_T$  and ( $\blacktriangle$ )  $k_{PT}$  in methylene chloride (MC); ( $\diamond$ )  $k_T$  in toluene (T). Excitation as in Figure 4.

band has a small fast component (0.2  $\mu\text{s}$ ), the remainder having time constant 1.7  $\mu\text{s}$ . With eq 3, this biphasic decay can be assigned to  $k_T^a$  and  $k_{PT}^b$ , respectively. At 273 K and below, observation of the rise of the 415-nm band allows unambiguous assignment of the rate constants (Figure 4A). The resulting fit of the 300 K point on the Arrhenius plot (Figure 5) confirms this interpretation of the two rate constants at 300 K. Activation energies are shown in Table II and rate constants in Table III.

**Toluene.** No 415-nm band is seen at any temperature nor is a faster component detectable in the 470-nm decay following excitation. The plot of ratios of absorbance changes at various wavelengths is time independent. The simplest interpretation is that the observed rate constant is that of electron transfer, followed by rapid decay to the ground state. Activation energies are shown in Table II and rate constants in Table III.

No definitive evidence for reaction of  $\text{PQ}_b$  was obtained in methylene chloride and toluene over the time scale studied. The observed yield of triplet in methylene chloride is constant between

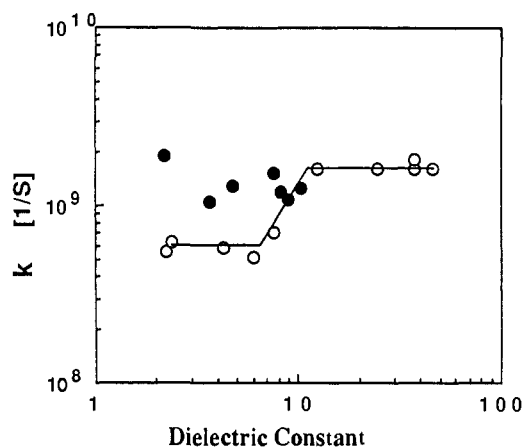


**Figure 6.** The logarithm of the electron-transfer rate constant of conformer a of  $\text{ZnPQ}(\text{Ac})_4$  is plotted versus the logarithm of the dielectric constant of the solvent at 300 K: ( $\circ$ ) nonchlorinated solvents and ( $\bullet$ ) chlorinated solvents. See Table I for data.

300 and 200 K, while this yield is calculated via fluorescence lifetimes to increase only 15%. The observed triplet yield in toluene increases 30% between 300 and 190 K, while this yield is calculated to increase by 20%. Thus the agreement between fluorescence and flash photolysis measurements is good in these as well as in the alcoholic solvent.

**Sucrose Octaacetate.** The lifetime of triplet  $\text{ZnPQ}(\text{Ac})_4$  in sucrose octaacetate at 300 K is only 13  $\mu\text{s}$ . No 415-nm band was observed.

## Discussion

Environmental effects on the rate constants for quenching of the singlet and triplet states of  $\text{ZnPQ}(\text{Ac})_4$  will be discussed followed by their effects on the equilibrium constant between the two conformers.

**1. Rate Constants.** The temperature independence of the quenching of the singlet state of the a, or small cavity, conformer of  $\text{ZnPQ}(\text{Ac})_4$ , first observed in dimethylacetamide-ethanol 1:1,<sup>13</sup> has now been measured in five solvents (Figures 1-3, Table II) having a wide range of physical properties: dielectric constant, polarizability, viscosity, and density. The near-zero activation energies are an intrinsic property of the porphyrin quinone complex not an accident of interaction with the solvent. The quenching involves electron transfer because it is strictly dependent on the presence of the quinone.<sup>13</sup> However, the lifetime of the ionized singlet state is unknown. Either the electron tunnels first and traps later,<sup>3</sup> or the charge-transfer reaction opens a fast channel to the ground state. If this new channel is faster than the solvent reorganization times, then either hypothesis could explain the near zero activation energies (Table II) and the striking lack of dependence on solvent dielectric relaxation time (Figures 2 and 3), including the large changes at the glass point. There is a weak dependence of  $k_a$  on the dielectric constant of the solvent (Figure 6), indicative of at least partial electron transfer. The dependence of  $k_b$ , or large cavity, conformer on solvent is somewhat more marked (Table I) as is the rate constant for the triplet state (Figure 5 and Table V of ref 13).

Observation of the porphyrin cation absorption at 415 nm provides clear evidence for the fully ionized state from triplet  $\text{ZnPQ}(\text{Ac})_4$  in polar solvents. However, since the free energy for this reaction is only about  $-0.2 \pm 0.1 \text{ eV}$  in polar solvents,<sup>13</sup> it is likely to become positive in nonpolar solvents. Indeed no evidence for ionization is obtained in nonpolar solvents, but the triplet lifetime is much shortened (Figure 5, Table III in ref 13). Even though no measurable amount of  $\text{P}^+\text{Q}^-$  is formed, the electronic coupling with this state may allow spin dephasing via nuclear and vibronic moments as the electrons are separated and the exchange interactions decrease. This opens a decay channel to the ground state. The virtual interaction with these higher energy ionic states need only be very weak to lead to quenching of the excited triplet state, since the lifetimes are so long:  $>10 \mu\text{s}$ . Quenching of excited

porphyrins by quinones in solution with unfavorable electron-transfer energetics has been observed,<sup>20</sup> including the present tetramethoxyquinone.<sup>13</sup> In agreement with this energy level argument, the free base derivative PQ(Ac)<sub>4</sub> is unreactive in either excited state.<sup>13</sup>

The small size, and changing sign, of the activation energies for the singlet and triplet reactions (Table II) are difficult to explain by adiabatic theories<sup>21</sup> of electron transfer. The near zero observed activation energies require a large reorganization energy,  $\geq 0.6$  eV. Moreover a fit to the rate constants as a function of free energy of reaction quoted in Table VIII of ref 13 requires a reorganization energy of  $\sim 1.2$  eV. Since the electrostatic solvation energies for the ionized state vary by 1.4 to 1 eV over this range of solvents with use of the Marcus two sphere<sup>22</sup> or the Onsager cavity model,<sup>23</sup> the consistently small activation energies pose a problem even admitting that these models overestimate the electrostatic energies. Only if one assumes the solvation energy contribution to the free energy of reaction and to the reorganization energy is identical together with the equality of the free energy in vacuo with the "internal" reorganization energy, can the observation of zero activation energy independent of solvent dielectric be explained. Hush<sup>24</sup> has proposed a particular model to minimize dependence on solvent. However, as pointed out by Suppan,<sup>25</sup> extensive prereorganization of a polar solvent is highly unlikely. We therefore conclude that only a nonadiabatic mechanism is viable.

The rate data can be explained by the nonadiabatic model of Kakitani and Kakitani<sup>26</sup> which is based on the radiationless transition theory of Lin.<sup>27</sup> Rate constants will have a small temperature dependence if the dominant vibronic mode coupling the excited and ionized states is larger than thermal energy. This mode could be the C-C and C-O vibrations (1600 cm<sup>-1</sup>) of porphyrins and quinones. A weak temperature dependence of either sign can arise from the thermal populations of modes which shift frequency between reactants and products. To produce the observed effects below the 300 K range, these modes must be of low frequency ( $\sim 200$  cm<sup>-1</sup>). These frequency shifts may well be of opposite signs: decreasing vibrational frequencies in the transition Q  $\rightarrow$  Q<sup>-</sup> but increasing frequencies in the solvation modes on ionization. The cancellation of effects can result in small residual activation energies which are difficult to predict but which may cause the variations seen in Table II.

A plot of the rate constant for electron transfer of PQ<sub>a</sub> versus the static dielectric constant of the solvent shows limiting values at both high and low dielectrics (Figure 6). A plot using the Onsager parameter<sup>23</sup> shows the same characteristics. The change between the limits occurs at a dielectric of about eight, which is also the value observed for changes of rate constants in other charge-transfer systems.<sup>28,29</sup> The rate limit at low dielectric constant (Figure 6) may be caused by the polarizable spacer units in the ZnPQ(Ac)<sub>4</sub> molecule. These spacers contribute to the dielectric of the local environment, i.e., that space which influences the tunneling wave functions, irrespective of the dielectric constant of the solvent. The static dielectric constant of the spacer units is estimated to be about 22 (equimolar mixture of anisole and dimethylacetamide), and the optical dielectric constant to be about 2.4 (equimolar mixture of 4-methyl anisole and *N*-methyl-*N*-

phenylacetamide, Table I). The former estimate may be somewhat high because of the limited motion of the benzanilide groups compared to the liquid motions of their surrogates. Given this reservation and the limited spatial extent of the spacers a leveling of the effective dielectric constant at  $\sim 8$  is not unreasonable. Therefore even in nonpolar solvents the local dielectric of ZnPQ(Ac)<sub>4</sub> may be  $\sim 8$ . Note that the optical dielectric constant of the spacer units is not affected by orientation relaxation (only a smaller anisotropic effect enters), and this dielectric is larger than that of any of the solvents in Table I. Because electron tunneling is favored in more polarizable material<sup>13</sup> the tunneling "path" will emphasize these spacer units. This does not mean that the tunneling is "through bonds".<sup>31</sup> The low energy of the electrons involved in these reactions,  $\sim 2$  eV, as compared to that of the empty solvent orbitals,  $\sim 6$  eV, disfavors the pathway involving overlap of the intervening large number of atomic orbitals.<sup>13</sup> Thus the ZnPQ(Ac)<sub>4</sub> molecule is sufficiently complex that it carries a considerable part of its environment along irrespective of solvent. We predict that the limiting electron-transfer rate would be the same in the vacuum or vapor state. As a corollary, changing the spacers should have a small effect on the rate, and this is observed (ref 13, Table III). In this way ZnPQ(Ac)<sub>4</sub> is closer to the bacterial photosynthetic reaction center, which has a completely self-contained enclosed environment, than to other open, linear, or partially closed porphyrin-quinone molecules.<sup>6</sup>

The rate constants  $k_a$  for heavily chlorinated solvents are larger than the correlation line of other solvents with the same dielectric constant (Figure 6). The average time constant for the four solvents containing the XCCl<sub>3</sub> (X = Cl, CHCl<sub>2</sub>, CH<sub>3</sub>) group is  $0.73 \pm 0.16$  ns, while that of solvents with the same dielectric constant but without chlorine atoms is  $1.6 \pm 0.2$  ns. Molecules with the XCCl<sub>3</sub> group cannot fit in the cavity of PQ<sub>a</sub>. A possible cause of this more rapid reaction is the increased filled orbital electron density outside of the PQ molecule in the solvent relative to the spacer units and polar cavidands. This increased electron density acts as an outside barrier, increasing the electron tunneling density in the interior of the cavity. The effect is just the opposite of the usual barrier picture of electron tunneling where the barrier is positioned between the donor and acceptor. We call this the tamper effect, and a detailed discussion is given in reference 32.

**2. Conformer Equilibrium.** There is a striking complementarity between the equilibrium constant  $K = \text{PQ}_a/\text{PQ}_b$  and the quenching rate constant of the large cavity conformer,  $k_b$ . This is seen in the temperature data in ethanol/methanol (Figure 2), methylene chloride (Figure 3, circles), and in other solvents at 300 K (Table I), e.g., acetonitrile. Arguments against the assumption that  $k_b$  is the conformer interconversion rate were given in the Experimental (data analysis) Section. The complementarity of  $K$  and  $k_b$  may be explained if the electron transfer in PQ<sub>b</sub> requires motion along the coordinate for interconversion of the two conformers. The activation energy of  $k_b$  is about half of the enthalpy of  $K$  (Table II) which is in agreement with this correlation which requires  $E_a < \Delta H$ . The motion may enhance the electron tunneling by increasing orbital overlap between the porphyrin and quinone through changes in both their distance and orientation.

The equilibrium constant for PQ<sub>a</sub> and PQ<sub>b</sub> is near unity, indicating little change in strain in either conformer. Solvent effects are small because no bonds or polarities are changed upon interconversion (Table I), but the *size* of the solvent molecule can alter the conformer equilibrium. Larger molecules will favor PQ<sub>b</sub> which has the larger cavity. A plot of log  $K$  versus molar volume of the solvent shows a general decrease in  $K$  with increasing solvent

(20) Connolly, J. S.; Hurlley, J. K. *Supramolecular Photochemistry*; Balzani, V., Ed.; Reidel, NATO ASI Series, 1987; Vol. 214, pp 299-318.

(21) Marcus, R. A.; Sutin, N. *Biochim. Biophys. Acta* **1985**, *811*, 265-322.

(22) Marcus, R. A. *J. Chem. Phys.* **1956**, *24*, 966. Bruntschwig, B. S.; Ehrenson, S.; Sutin, N. *J. Phys. Chem.* **1986**, *90*, 3657-3668.

(23) Onsager, L. *J. Am. Chem. Soc.* **1963**, *58*, 1486-1493.

(24) Hush, N. S. In *Supramolecular Photochemistry*; Balzani, V., Ed.; D. Reidel: 1987; pp 53-72.

(25) Suppan, P. *Chimia* **1988**, *42*, 320-330.

(26) Kakitani, T.; Kakitani, H. *Biochim. Biophys. Acta* **1981**, *635*, 498-514.

(27) Lin, S. H. *J. Chem. Phys.* **1966**, *44*, 3759-3767.

(28) Weller, A.; Zacharias, K. *Chem. Phys. Lett.* **1971**, *10*, 590-594.

(29) The failure to measure faster rates is not a function of our fluorescence lifetime apparatus: lifetimes down to 60 ps have been measured with porphyrin-bisquinone cyclophanes with a closer porphyrin-to-quinone separation.<sup>30</sup>

(30) Mauzerall, D.; Weiser, J.; Staab, H. *Tetrahedron* **1989**, *45*, 4807-4814.

(31) Oevering, H.; Paddon-Row, M. N.; Heppener, M.; Oliver, A. M.; Cotsaris, E.; Verhoeven, J. W.; Hush, N. S. *J. Am. Chem. Soc.* **1987**, *109*, 3258-3269.

(32) Delaney, J.; Mauzerall, D. *Photosynth. Res.* **1989**, *22*, 197-201.

(33) Riddick, J. A.; Bunger, W. B.; Sakano, T. K. *Organic Solvents*, 4th ed.; Wiley-Interscience: New York, 1986.

(34) Maryott, A. A.; Smith, E. R. Table of Dielectric Constants of Pure Liquids. *Natl. Bur. Stand. Circ. (U.S.)* **1951**, *514*, 5.

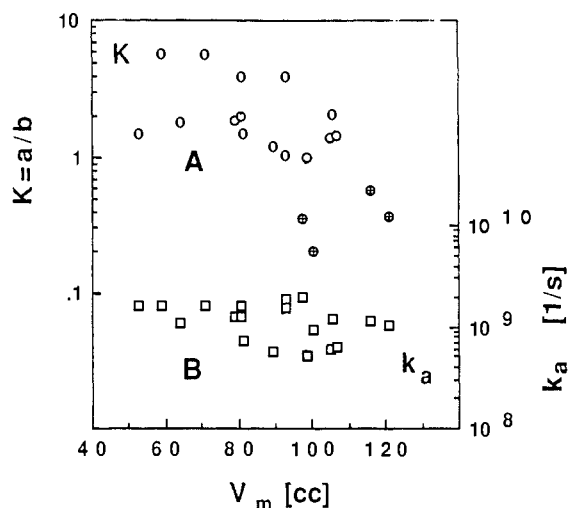


**Figure 7.** (A) The logarithm of the equilibrium constant for the conformers of  $\text{ZnPQ}(\text{Ac})_4$  at 300 K (O) is plotted versus the molar volume of the solvent. The points on the left edge are molecules close to spherical (e.g., benzene), whereas those on the right edge are more elliptical (e.g., diethyl ether). The symbol  $\oplus$  indicates hexafluorobenzene,  $\text{CH}_2\text{Cl}_2$ ,  $\text{CHCl}_2\text{CCl}_3$ , and  $\text{CCl}_4$ . (B) The logarithm of the rate constant  $k_a$  ( $\square$ ) is plotted versus the molar volume of the solvent. See Table I for data.

size (Figure 7A), albeit with some scatter. A plot of  $\log k_a$  in the same manner shows no such correlation (Figure 7B). The molecules on the left edge of the scatter zone of the  $\log K$  plot are close to spherical ( $\text{CH}_3\text{CN}$ ,  $\text{PhH}$ ,  $\text{CCl}_4$ ). If the minimum axis of the more ellipsoidal molecules are used as a volume measure,

the points on the right edge of the zone shift horizontally to smaller volumes, decreasing the scatter. It is striking that the solvents with  $K < 1$  (crossed circles) are hexafluorobenzene or contain the  $\text{XCCl}_3$  group with  $\text{X} = \text{Cl}$ ,  $\text{CHCl}_2$ , or  $\text{CH}_3$ . Molecular models indicate that such molecules are too large to fit in the cavity of  $\text{PQ}_a$ . Assuming the molar volume at  $K = 1$  (100 cc in Figure 7A) defines the size of the cavity, the radius of the equivalent sphere is 3.4 Å. This is just the spacing estimated for the cavity in  $\text{PQ}_a$ .<sup>13</sup>

### Conclusion

The weak solvent dependence and the temperature independence of the electron-transfer reactions of  $\text{ZnPQ}(\text{Ac})_4$  are best interpreted by nonadiabatic electron tunneling. The somewhat larger dependencies of the triplet state reactions are explained by the closeness of the energy levels of the triplet state and that of  $\text{ZnP}^+\text{Q}^-(\text{Ac})_4$ : 1.6 eV and 1.4 eV in polar solvents. Thus over 90% of the energy of this state is converted to free energy of the products.

Although the complexity of this macropolycyclic porphyrin-quinone cage molecule causes difficulties in the kinetic analysis of its electron-transfer reactions, this complexity is also a source of valuable information on the parameters which control the rate of these reactions. The polarizable spacer groups holding the porphyrin-quinone molecule together both isolate the reactants from the environment and favor the reaction, as in the photosynthetic reaction center.

**Acknowledgment.** We thank Professor Henry Linschitz for very useful advice and for critical comments on this manuscript. This research was supported by the National Science Foundation, (DMB83-16373 and DMB87-18078) and by the Rockefeller University.

## Determination of a Precise Interatomic Distance in a Helical Peptide by REDOR NMR

Garland R. Marshall,<sup>\*,†</sup> Denise D. Beusen,<sup>†</sup> Karol Kocielek,<sup>†,‡</sup> Adam S. Redlinski,<sup>†,‡</sup> Mirosław T. Leplawy,<sup>†,‡</sup> Yong Pan,<sup>§</sup> and Jacob Schaefer<sup>§</sup>

Contribution from the Department of Pharmacology, Washington University School of Medicine, St. Louis, Missouri 63110, Institute of Organic Chemistry, Politechnika, Lodz, Poland, and Department of Chemistry, Washington University, St. Louis, Missouri 63130.  
Received March 13, 1989

**Abstract:** A new spectroscopic technique, rotational-echo double-resonance (REDOR) NMR, for solids utilizes magic-angle spinning and measures directly the dipolar coupling between stable-isotope-labeled nuclei and, thus, interatomic distances. REDOR has been used to measure the  $^{13}\text{C}$ - $^{15}\text{N}$  interatomic distance in a nine-residue fragment, Ac-Phe-MeA( $1\text{-}^{13}\text{C}$ )-MeA( $d_6$ )-MeA-Val-Gly( $^{15}\text{N}$ )-Leu-MeA-MeA-OBzl (MeA =  $\alpha$ -methylalanine or aminoisobutyric acid (Aib)), of the peptide antibiotic emerimicin. The crystal structure of the peptide emerimicin 1-9 benzyl ester was determined previously, and the measurement by REDOR of a known interatomic distance allows both validation and a practical demonstration of the precision of REDOR. The ability to map precisely intermolecular distances suggests applications of REDOR in the solid, or aggregated state, for determinations of the conformations of ligand molecules in drug-receptor, inhibitor-enzyme, and antigen-antibody complexes.

Recent advances in NMR technology have allowed the determination in solution of the three-dimensional structure of small proteins at low resolution.<sup>1,2</sup> These techniques are based primarily on measurements of proton homonuclear nuclear Overhauser effects (NOE's). NOE-based methods for distance determination

suffer a number of shortcomings, among them the need to approximate a specific correlation time in the context of a model of microscopic motion. While the range for determining interproton distances by NOE may extend to 5 Å, the error range is also large. Only by iteratively fitting the calculated structures to the experimental data can this range be reduced to  $\pm 10\%$ . The

\* To whom correspondence should be addressed.

† Washington University School of Medicine.

‡ Guest investigators, Politechnika.

§ Washington University.

(1) Wuthrich, K. *Science* 1989, 243, 45.

(2) Clore, G. M.; Gronenborn, A. M. *Protein Eng.* 1987, 1, 275.